

Ultrathin porous NiO nanoflake arrays on nickel foam as an advanced electrode for high performance asymmetric supercapacitors

Shuxing Wu,^a K.S. Hui,^{*b} K.N. Hui^{*c} and Kwang Ho Kim^{*ad}

^aSchool of Materials Science and Engineering, Pusan National University, San 30 Jangjeon-dong, Geumjeong-gu, Busan 609-735, Republic of Korea

^bDepartment of Mechanical Convergence Engineering, Hanyang University, 17 Haengdang-dong, Seongdong-gu, Seoul 133-791, Republic of Korea

^cInstitute of Applied Physics and Materials Engineering, University of Macau, Avenida da Universidade, Taipa, Macau, China

^dGlobal Frontier R&D Center for Hybrid Interface Materials, Pusan National University, 30 Jangjeon-dong, Geumjung-gu, Busan 609-735, South Korea

**Corresponding author:*

E-mail: kshui@hanyang.ac.kr (*Kwan San Hui*)

Tel: +82 2-2220-0441; *Fax:* +82 2-2220-2299

E-mail: bizhui@umac.mo (*Kwun Nam Hui*)

Tel: +853 8822-4426; *Fax:* +853 8822-2426

E-mail: kwhokim@pusan.ac.kr (*Kwang Ho Kim*)

Tel.: +82 51-510 3391; *Fax:* +82 5-1514-4457

Preparation of reduced graphene oxide (rGO) electrode

Graphite oxide (GO) was synthesized from graphite powder (Sigma-Aldrich) using a modified Hummers method.¹ The rGO was prepared by applying thermal expansion of the as-fabricated GO powder at 1050 °C for 30 s in an Ar atmosphere.² The rGO electrode was prepared according to our previous work.³ Briefly, 85 wt% of rGO was mixed with 10 wt% acetylene black and 5 wt% polytetrafluoroethylene (PTFE). Then resulting mixture was coated onto the nickel foam (1 cm × 1 cm). After pressing under a pressure of 20 MPa, the electrode was dried at 80 °C overnight in a vacuum oven. The mass loading for rGO electrode was determined by comparing the mass difference between the original nickel foam and the nickel foam coated with mixture.

Calculations

For the two-electrode system, the charge balance between the two electrodes satisfy the relationship of $q^+ = q^-$ (q^+ is the positive charge and q^- is the negative charge). The charge stored by each electrode follows the equation:⁴

$$q = C \times \Delta V \times m \quad (\text{S1})$$

where C (F g^{-1}) is the specific capacitance from cyclic voltammetry (CV) curves, ΔV (V) is the potential window, and m (g) is the mass of the electrode. The mass ratio between the positive and negative electrodes was calculated based on the following equation:⁵

$$\frac{m_+}{m_-} = \frac{C_- \times \Delta V_-}{C_+ \times \Delta V_+} \quad (\text{S2})$$

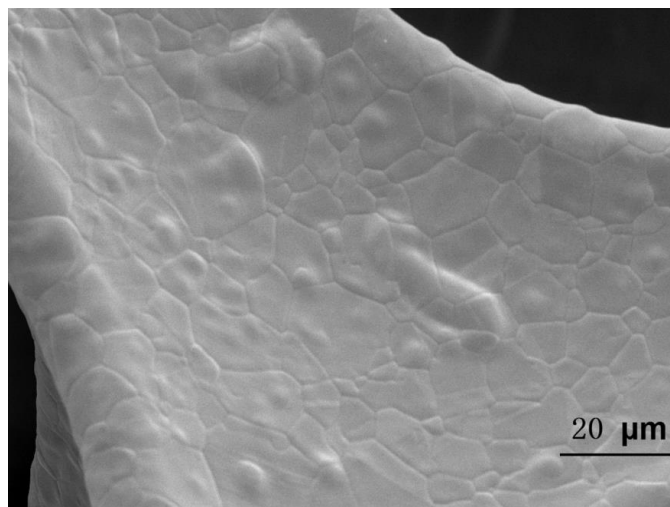


Fig. S1 SEM images of fresh nickel foam.

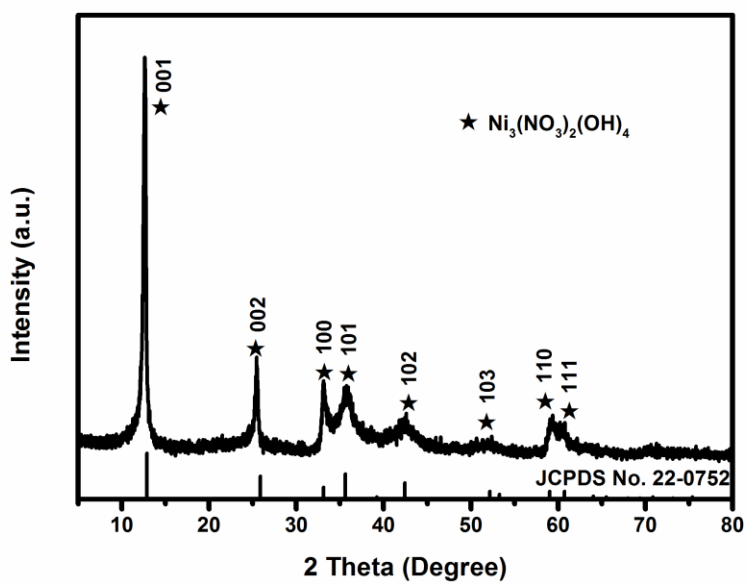


Fig. S2 XRD patterns of $\text{Ni}_3(\text{NO}_3)_2(\text{OH})_4$ nanoflakes.

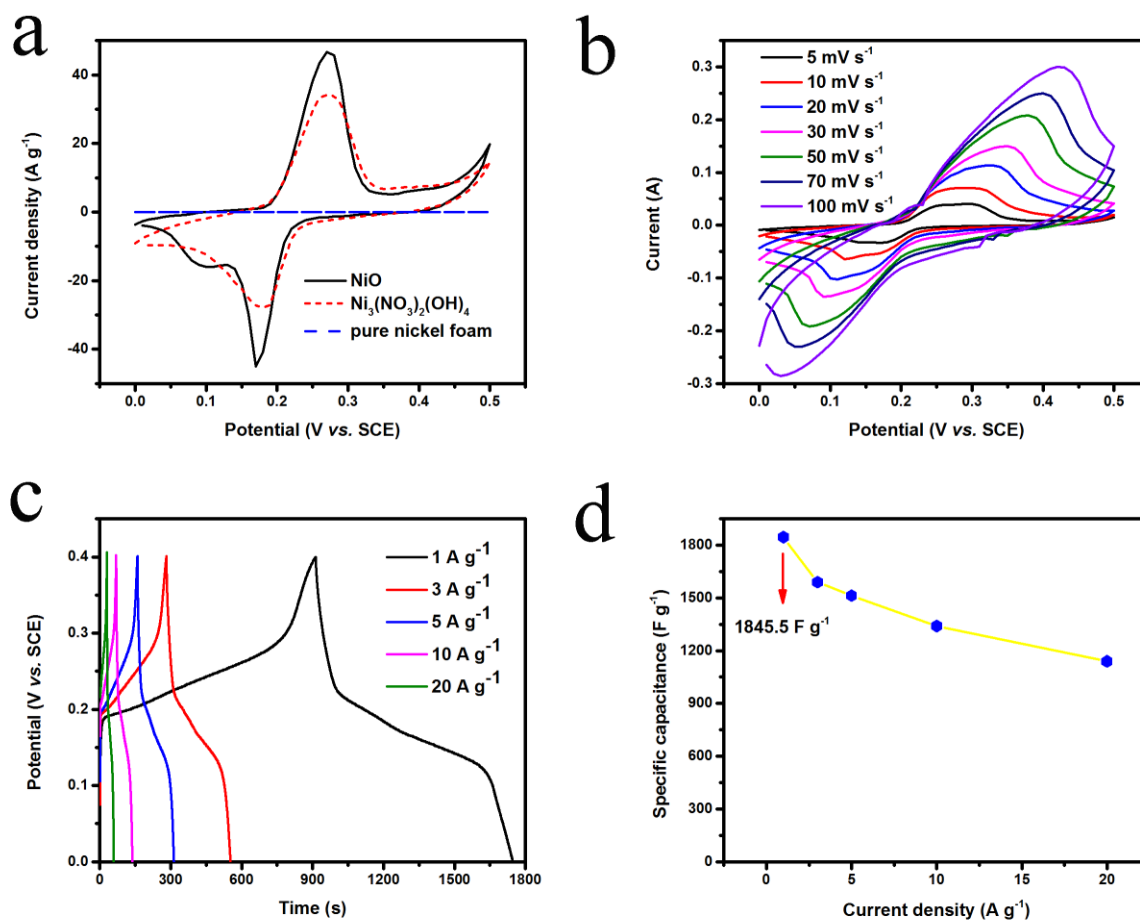


Fig. S3 Three-electrode electrochemical measurements of $\text{Ni}_3(\text{NO}_3)_2(\text{OH})_4$ nanoflakes electrode in a 6 M aqueous solution: (a) CV curves of pure NiO nanoflakes, $\text{Ni}_3(\text{NO}_3)_2(\text{OH})_4$ nanoflakes and nickel foam at 5 mV s^{-1} . (b) CV curves of the NiO nanoflakes electrode at various scan rates. (c) Constant current discharge curves of NiO nanoflakes electrode at different current densities. (d) Rate capability of the NiO electrode at various current densities.

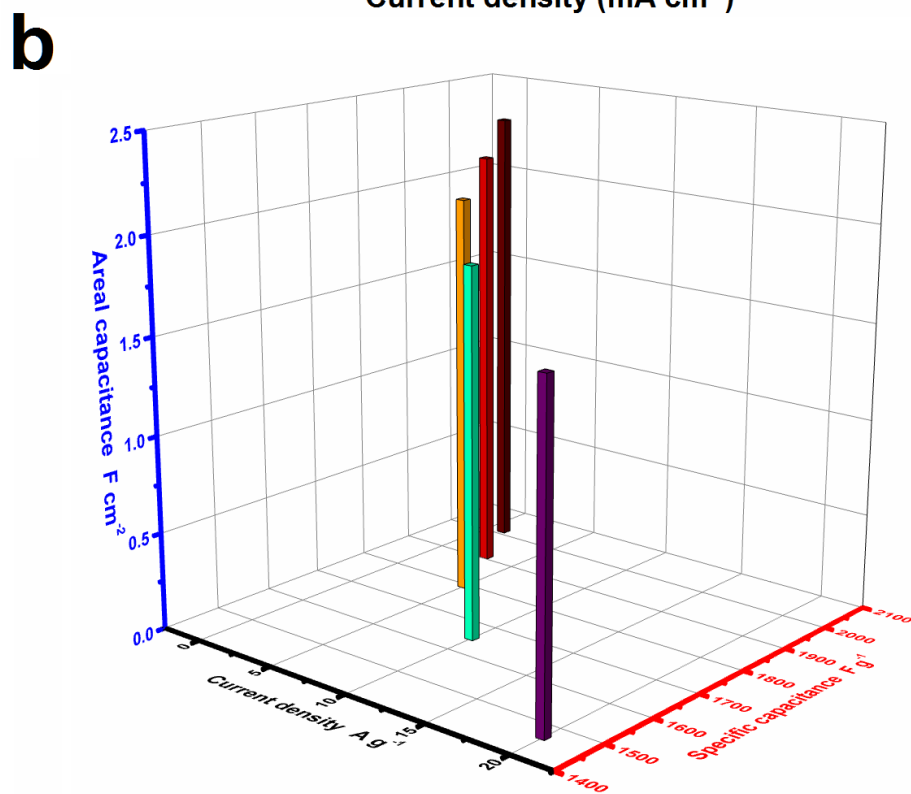
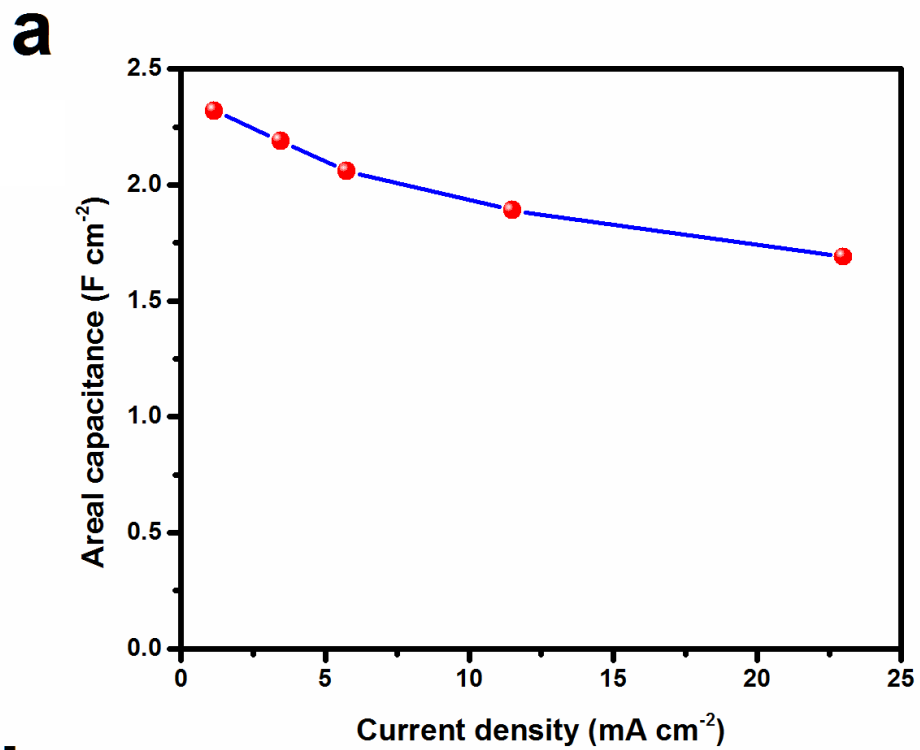


Fig. S4 (a) Current density dependence of the areal capacitance. (b) Areal and gravimetric capacitances vs current density.

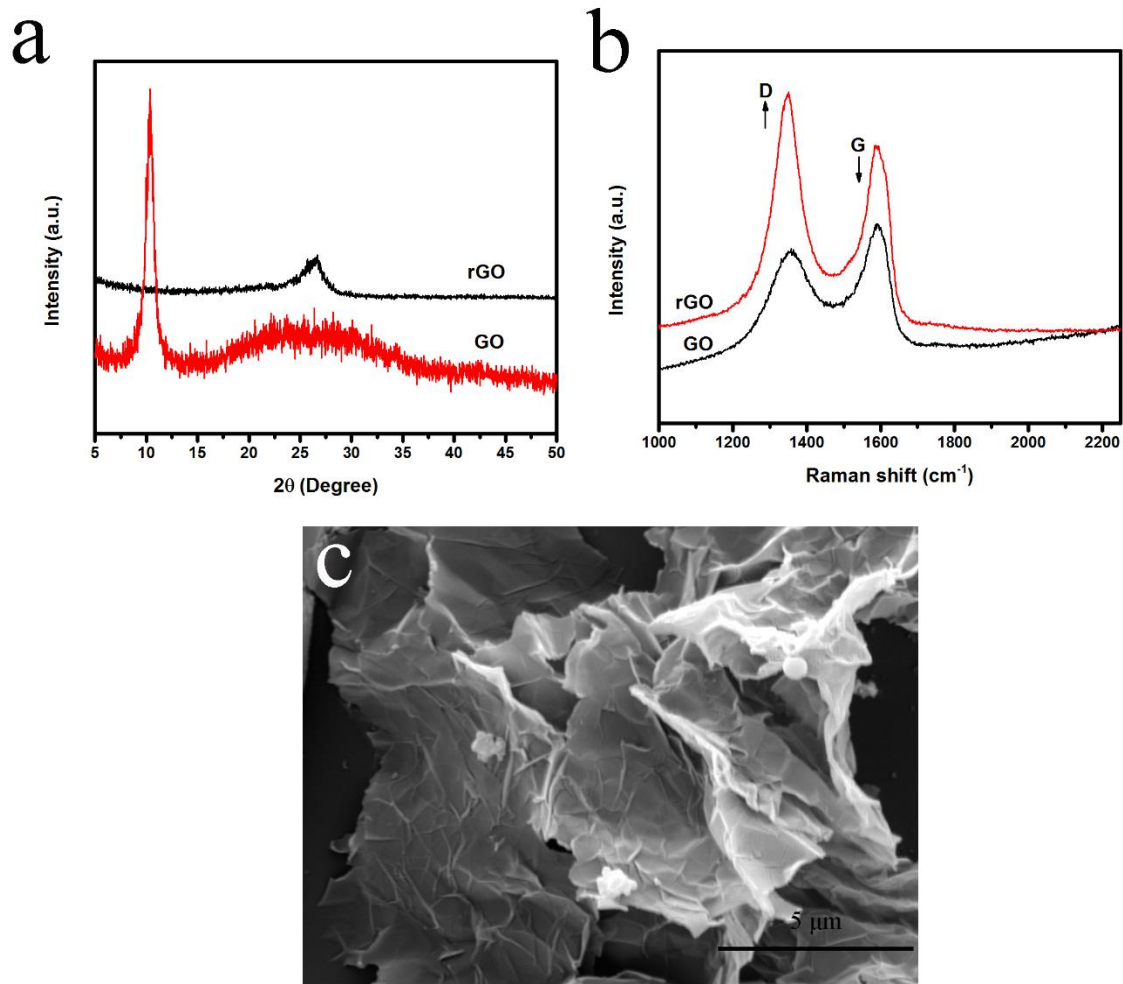


Fig. S5 (a) Powder XRD pattern of GO and rGO. (b) Raman spectra of GO and rGO. (c) SEM image of rGO.

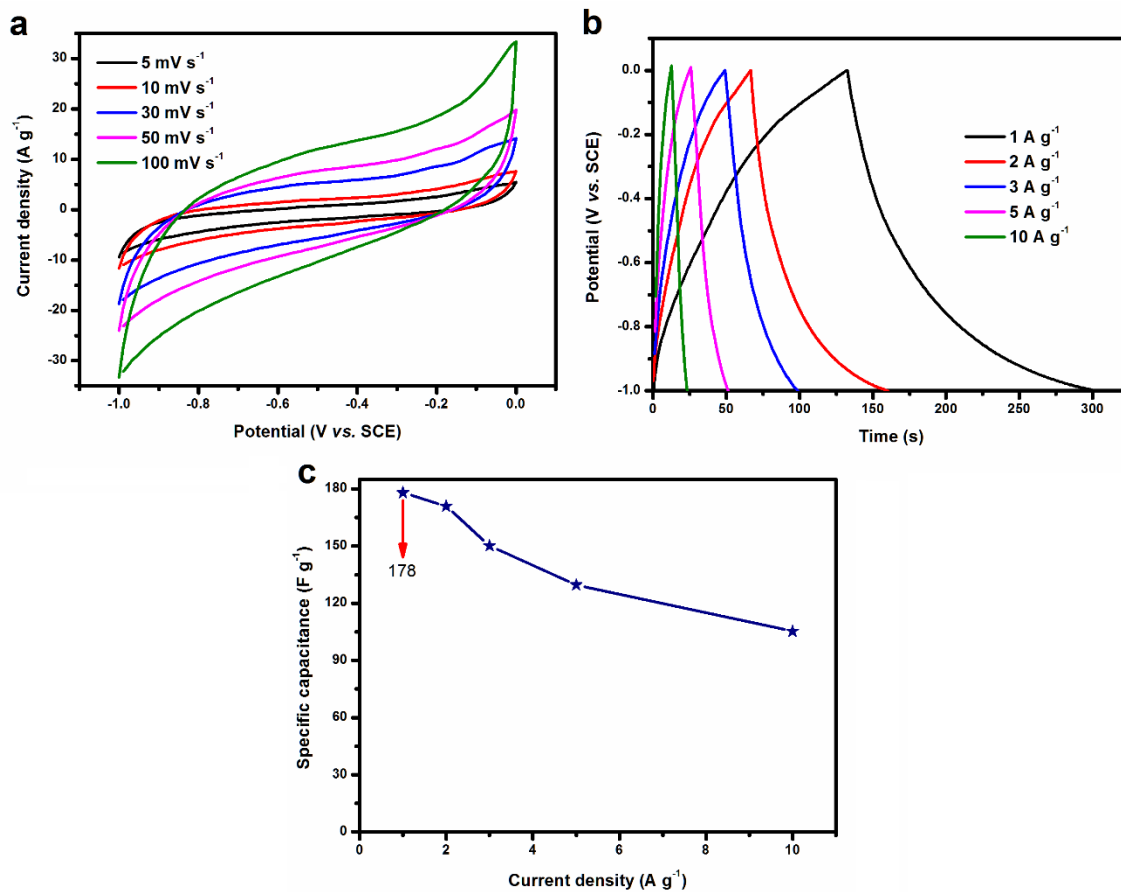


Fig. S6 Electrochemical performance of the rGO as supercapacitor electrodes in the three-electrode measurements in 6 M KOH electrolyte. (a) CV curves at various scan rates; (b) GCD curves under different current densities; (c) Summary of specific capacitance as a function of current density.

Table S1 EIS fitting parameters of ultrathin porous NiO nanoflakes

R_s (Ω)	R_{ct} (Ω)	C_{dl} (F)	W ($\Omega s^{-1/2}$)	C_F (F)
0.435	0.125	0.000395	0.320	0.0487

Table S2 Comparison of the electrochemical performance of the NiO electrode with those in previous reports

Ref.	Material	Preparation method	Electrolyte	Specific capacitance (F/g)	Rate performance	Capacitance retention (cycles)
This work	NiO nanoflake on nickel foam	Solvothermal-annealing	6 M KOH	2013.7 (1 A/g)	72.8% (20 A/g)	100% (5000)
6	NiO nanoflake on nickel foam	Chemical bath deposition	5 M KOH	268 (2 A/g)	79.8% (10A/g)	\
7	NiO nanowire@NiO nanosheet on nickel foam	Hydrothermal	6 M KOH	1349 (5 A/g)	58% (50 A/g)	87% (2000)
8	NiO nanoplatelet arrays on nickel foam	Precipitating hydroxides+calcinating	6 M KOH	1124 (2 A/g)	77% (16 A/g)	97% (5000)
9	Mesoporous NiO nanoflake array on nickel foam	Hydrothermal	2 M KOH	400 (2 A/g)	84.8% (40 A/g)	107% (5000)
10	Porous NiO film on nickel foam	Chemical bath deposition	1 M KOH	279 (2 A/g)	84.3% (40 A/g)	87% (2000)
11	Porous NiO nanotube arrays on nickel foam	Electrodeposition-etching	2 M KOH	675 (2 A/g)	67.4% (40 A/g)	93.2% (1000)
12	NiO nanorod arrays on nickel foam	Hydrothermal	1 M NaOH	2018 (2.27 A/g)	76.1% (22.7 A/g)	92% (500)
13	NiO nanoarrays on nickel foam	In suit growth	6 M KOH	2065 (16 A/g)	60.4% (70 A/g)	88.9% (5000)
14	NiO nanosheet on nickel foam	In suit growth	2M KOH	2504.3 (13.4 A/g)	71.4% (134.2 A/g)	100% (45000)
15	NiO nanoparticles on nickel foam	Electrodeposition	1 M KOH	2558 (2 A/g)	70% (40 A/g)	74% (1000)

References

1. N. I. Kovtyukhova, P. J. Ollivier, B. R. Martin, T. E. Mallouk, S. A. Chizhik, E. V. Buzaneva and A. D. Gorchinskiy, *Chem Mater*, 1999, **11**, 771-778.
2. S. Zhang, J. Niu, H. H. Song, L. X. Zhu, J. S. Zhou, X. H. Chen, J. Z. Liu, S. Hong and R. R. Song, *J Mater Chem A*, 2013, **1**, 14103-14107.
3. S. X. Wu, K. S. Hui and K. N. Hui, *J Phys Chem C*, 2015, **119**, 23358-23365.
4. L. Q. Mai, A. Minhas-Khan, X. C. Tian, K. M. Hercule, Y. L. Zhao, X. Lin and X. Xu, *Nat Commun*, 2013, **4**, 2923.
5. S. Narayanan, J. R. Hajzus, C. E. Treacy, M. R. Bockstaller and L. M. Porter, *J. Solid State Sci Tech*, 2014, **3**, P363-P369.
6. C. H. Wu, S. X. Deng, H. Wang, Y. X. Sun, J. B. Liu and H. Yan, *Acs Appl Mater Inter*, 2014, **6**, 1106-1112.
7. L. An, K. B. Xu, W. Y. Li, Q. Liu, B. Li, R. J. Zou, Z. G. Chen and J. Q. Hu, *J Mater Chem A*, 2014, **2**, 12799-12804.
8. C. Z. Yuan, J. Y. Li, L. R. Hou, L. Yang, L. F. Shen and X. G. Zhang, *Electrochim Acta*, 2012, **78**, 532-538.
9. X. Y. Yan, X. L. Tong, J. Wang, C. W. Gong, M. G. Zhang and L. P. Liang, *J Alloy Compd*, 2014, **593**, 184-189.
10. X. H. Xia, J. P. Tu, Y. J. Mai, R. Chen, X. L. Wang, C. D. Gu and X. B. Zhao, *Chem-Eur J*, 2011, **17**, 10898-10905.
11. F. Cao, G. X. Pan, X. H. Xia, P. S. Tang and H. F. Chen, *J Power Sources*, 2014, **264**, 161-167.
12. X. J. Zhang, W. H. Shi, J. X. Zhu, W. Y. Zhao, J. Ma, S. Mhaisalkar, T. L. Maria, Y. H. Yang, H. Zhang, H. H. Hng and Q. Y. Yan, *Nano Res*, 2010, **3**, 643-652.
13. F. B. K. Velusamy Senthilkumar , Nhu Thuy Ho , Ji-Woong Kim , Sungkyun Park , Jong-Seong Bae , Won Mook Choi b, Shinuk Cho , Yong Soo Kim, *J Power Sources*, 2016, **303**, 363-371.
14. G. H. Cheng, W. F. Yang, C. Q. Dong, T. Y. Kou, Q. G. Bai, H. Wang and Z. H. Zhang, *J Mater Chem A*, 2015, **3**, 17469-17478.
15. H. W. Wang, H. Yi, X. Chen and X. F. Wang, *Electrochim Acta*, 2013, **105**, 353-361.